ADVANCED ELECTRONIC MATERIALS
www.advelectronicmat.de

Graphdiyne Filter for Decontaminating Lead-Ion-Polluted Water

Rong Liu, Jingyuan Zhou, Xin Gao, Jiaqiang Li, Ziqian Xie, Zhenzhu Li, Shuqing Zhang, Lianming Tong, Jin Zhang,* and Zhongfan Liu**

The decontamination of water polluted with heavy metal ions is of worldwide concern. Among various treatment approaches to remove metal ions from water, adsorption is regarded as an efficient method, and a variety of materials have been applied as adsorbents for the removal of metal ions from polluted water. Recently, carbon nanomaterials have been examined as alternative adsorbents due to their high specific surface areas, high removal efficiency, and strong interactions with metal ions. Graphdiyne, a new kind of carbon allotrope composed of sp- and sp^2-hybridized carbon atoms, has attracted great interest due to its impressive properties. Graphdiyne is considered to be a promising candidate for the adsorption of heavy metal ions as the acetylenic links in graphdiyne strongly interact with metal ions. Herein, graphdiyne is used as an adsorbent to remove lead ions from water. The interaction between lead ions and graphdiyne is explored by X-ray photoelectron spectroscopy and Raman spectroscopy. The maximum adsorption capacity calculated by the Langmuir isotherm model is 470.5 mg g^{-1}. Graphdiyne is also synthesized on copper foam and used as a filter to eliminate lead ions from water. The filter shows high performance with a removal efficiency of 99.6% and can be recovered through treatment with acidic solution.

Heavy-metal-contaminated wastewater is one of the most concerning environmental problems, as heavy metals are detrimental to human health as well as the entire ecosystem due to their toxicity, non-biodegradability, and accumulation in biological systems. Therefore, developing efficient methods to remove metal ions from polluted water before being released into the environment is essential. Various techniques have been applied to eliminate heavy metals, such as chemical precipitation,[1,2] ion exchange,[3,4] adsorption,[5] electrochemical treatment,[6] and membrane filtration.[7] Among these methods, adsorption is considered to be an effective and widely used strategy with numerous advantages, such as generality, high efficiency, relatively low cost, and possible regeneration of the adsorbent. Adsorption is realized through van der Waals forces, electrostatic attraction, ion exchange, or chemical binding between metal ions and adsorbents. Much effort has been made to develop new adsorbents and improve the performance of existing adsorbents. Recently, carbon materials, such as active carbons,[8] graphene,[9] and carbon nanotubes,[10] have been regarded as promising candidates for the adsorption of heavy metal ions due to their high specific surface areas and strong interactions with metal ions. The adsorption capacity of these carbon materials toward metal ions can be significantly increased through oxidation.[11,12]

Graphdiyne is a new 2D carbon material that is composed of sp- and sp^2-hybridized carbon atoms.[13,14] This material has attracted great attention due to its impressive properties, such as high carrier mobility,[15] high nonlinear optical susceptibility,[16] low thermal conductivity,[17] and uniformly distributed pores, which are defined by the atomic structure of graphdiyne. Graphdiyne has been proposed as a promising material for application in electronic devices, energy storage,[18] gas separation,[19,20] metal-free catalysis,[21] water purification,[22,23] etc. A number of studies have examined the synthesis of this material, and graphdiyne with different morphologies[24–27] and oligomeric subunits of graphdiyne[13,28] have been achieved. Various applications of these materials have been demonstrated by taking advantage of the electrical conductivity, hole-transport properties, and morphological characteristics of graphdiyne.[29–32] The acetylenic links in graphdiyne strongly interact with metal ions (**Figure 1**a), which can be utilized to adsorb metal ions from water. This material shows a different manner of adsorption than that of carbon adsorbents examined in previous work, in which oxygen-containing groups are generally regarded as the adsorption sites. Herein, we present the almost complete removal of lead ions from water by using a

R. Liu, J. Y. Zhou, X. Gao, Z. Q. Xie, Z. Z. Li, S. Q. Zhang, Prof. L. M. Tong, Prof. J. Zhang, Prof. Z. F. Liu
Center for Nanochemistry
Beijing Science and Engineering Center for Nanocarbons
Beijing National Laboratory for Molecular Sciences
College of Chemistry and Molecular Engineering
Peking University
Beijing 100871, P. R. China
E-mail: tonglm@pku.edu.cn; jinzhang@pku.edu.cn; zfliu@pku.edu.cn
R. Liu, J. Y. Zhou, Z. Z. Li, S. Q. Zhang
Academy for Advanced Interdisciplinary Studies
Peking University
Beijing 100871, P. R. China
J. Q. Li
School of Chemistry and Chemical Engineering
Chongqing University
Chongqing 400044, P. R. China

DOI: 10.1002/aelm.201700122

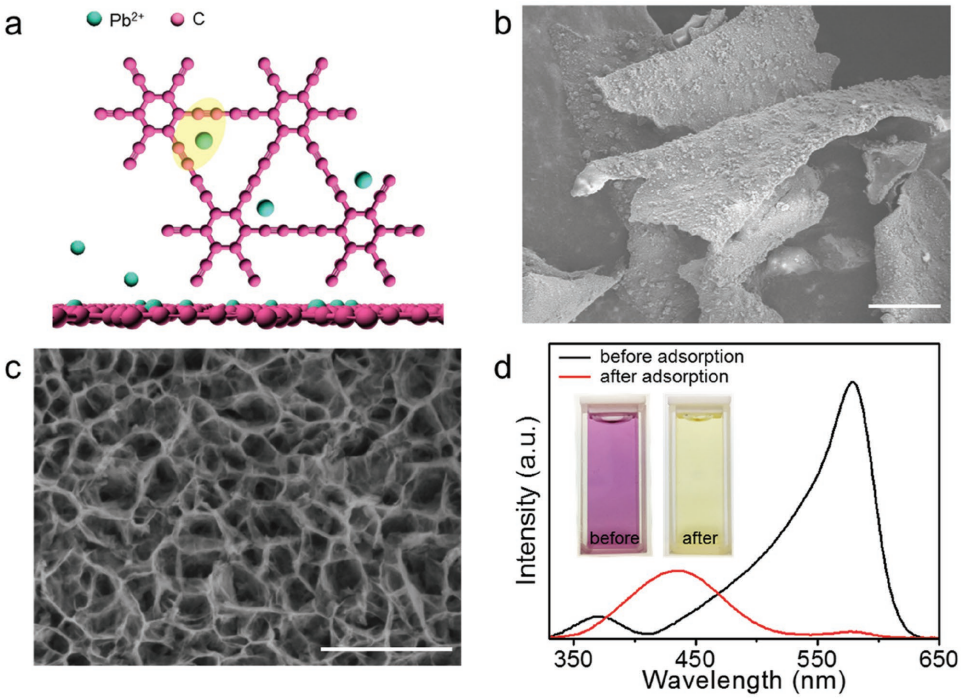

Figure 1. a) Schematic diagram showing the adsorption of lead ions on graphdiyne. b) SEM image of graphdiyne. Scale bar is 20 µm. c) High-magnification SEM image of graphdiyne, showing the nanowall structure. Scale bar is 1 µm. d) Absorption spectra of an aqueous solution containing lead ions with added xylenol orange before and after adsorption. Inset: photographs of the aqueous solution containing lead ions with added xylenol orange before and after adsorption.

graphdiyne-based filter. X-ray photoelectron spectroscopy (XPS) and Raman spectroscopy were used to explore the interaction between lead ions and graphdiyne. The change in the Raman peaks corresponding to the conjugated diyne links in graphdiyne after adsorption demonstrated that the acetylenic links in graphdiyne served as adsorption sites during the adsorption process. The maximum adsorption capacity calculated by the Langmuir isotherm model was 470.5 mg g^{-1}. In addition, graphdiyne synthesized on 3D highly porous copper foam can be used directly as a filter to remove lead ions from water. The filter showed a removal efficiency as high as 99.6% for a 4.8 mg L^{-1} solution of lead ions in water. Effects of the solution volume, initial lead ion concentration and number of filter operations on the filtration performance were also investigated. Moreover, the filter can be recovered through treatment with an acidic solution. The graphdiyne-based filter showed no obvious degradation in performance over eight repetitions.

Graphdiyne was synthesized on copper foil according to the method outlined in our previous report.[27] Details are presented in the Experimental Section in the Supporting Information. The copper substrates were removed with ferric chloride ($FeCl_3$, 1 M), and the remaining products were collected. The Raman spectrum of graphdiyne exhibited three typical Raman peaks (Figure S1, Supporting Information). The peak at 1398 cm^{-1} corresponds to the breathing vibration of the aromatic ring (D band), while the peak at 1578 cm^{-1} corresponds to the first-order scattering of the E_{2g} mode for the in-plane stretching vibration of sp^2 atoms (G band). In addition, the peak at 2175 cm^{-1} is attributed to the C≡C stretching mode in conjugated diyne, revealing the conversion of monomers to graphdiyne through the coupling reaction and confirming the successful synthesis of graphdiyne.[27,33] The morphology of the as-prepared graphdiyne powder was characterized by scanning electron microscopy (SEM). As shown in Figure 1b and Figure S2 (Supporting Information), the graphdiyne powder exhibits a plate-like morphology with a thickness of ≈700 nm. The high-magnification SEM image of graphdiyne (Figure 1c) shows the appearance of vertically erected nanowalls with voids of a few hundred nanometers in diameter. The specific surface area of the graphdiyne powder was calculated to be 104.9 m^2 g^{-1} by Brunauer–Emmett–Teller surface area analysis (Figure S3, Supporting Information).

To investigate the capability of removing metal ions from polluted water, graphdiyne powder was added into a $Pb(NO_3)_2$ aqueous solution with a certain concentration. The mixture was stirred for 24 h and then filtered through a microfiltration membrane to remove the graphdiyne powder from solution. The removal of lead ions can be visualized by adding xylenol orange into the aqueous solution before and after adsorption (Figure 1d, inset). Xylenol orange is a sensitive colorimetric indicator for the presence of many heavy metal ions in solution, showing yellow in pure water but turning to red in the presence of lead ions.[34] The corresponding absorption spectra are also shown in Figure 1d. Compared to the spectrum recorded before adsorption, the spectrum of the solution after adsorption shows a decrease in absorbance at ≈580 nm and a consequent increase in absorbance at ≈435 nm, which is consistent with the spectral features of blank xylenol orange.[35] This change in the spectrum confirms the removal of lead ions from water.

To investigate the adsorption mechanism of graphdiyne, XPS and Raman scattering were performed. **Figure 2**a shows

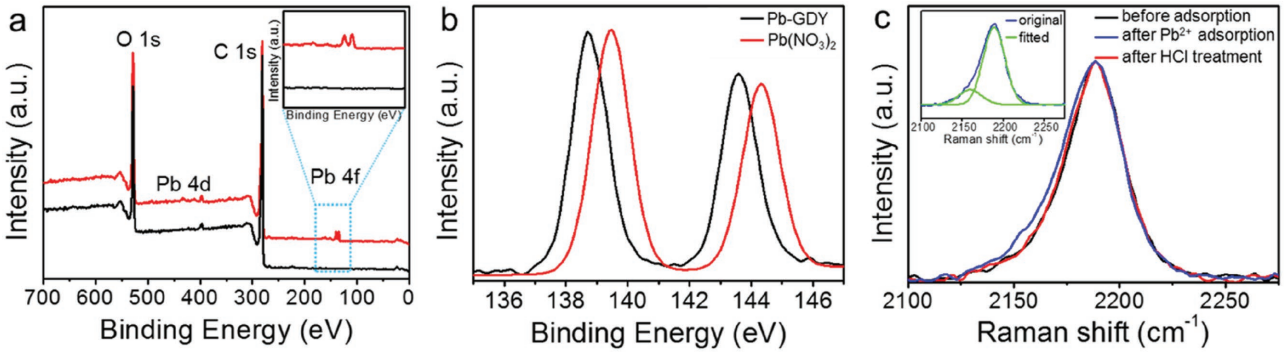

Figure 2. a) XPS survey spectra of graphdiyne before (black curve) and after (red curve) lead ion adsorption. b) High-resolution Pb 4f XPS spectra of $Pb(NO_3)_2$ (red curve) and lead ion-adsorbed graphdiyne (black curve). c) Raman spectra of the conjugated diyne links obtained from graphdiyne before lead ion adsorption (black curve), after lead ion adsorption (blue curve), and after treatment with HCl (red curve). Inset: curve fitting of the Raman spectrum after lead ion adsorption.

the XPS spectra obtained from graphdiyne before (black curve) and after (red curve) lead ion adsorption. After adsorption, a new pair of peaks at a binding energy of ≈140 eV, attributed to Pb 4f, appeared, which indicates the successful adsorption of lead ions on graphdiyne. The high-resolution Pb 4f XPS spectra of $Pb(NO_3)_2$ (red curve) and lead ions adsorbed on graphdiyne (black curve) are shown in Figure 2b. The two peaks can be assigned to Pb $4f_{7/2}$ and Pb $4f_{5/2}$, respectively. The Pb 4f binding energies of lead ions adsorbed on graphdiyne were clearly down-shifted by 0.7 eV compared to those of $Pb(NO_3)_2$. The decrease in binding energies provides direct evidence that lead ions received electrons from graphdiyne and indicates the strong binding of lead ions to graphdiyne, mainly attributed to interactions between lead ions and the sp-hybridized carbon atoms in graphdiyne. Due to the sp hybridization, graphdiyne presents not only out-of-plane p_z π/π^* orbitals (z is the direction perpendicular to the graphdiyne plane) but also in-plane $p_{x/y}$ π/π^* orbitals, which enables the π/π^* orbitals to rotate toward any direction perpendicular to the line of −C≡C−.[36] When metal atoms approach the surface of graphdiyne, the electrons from the metal atoms couple with the p_z orbitals as well as the p_x or p_y orbitals of the sp-hybridized carbon atoms, resulting in strong interactions between graphdiyne and the metal ions. To further examine this interaction, the Raman spectrum of graphdiyne was measured before and after the adsorption of lead ions. Figure 2c shows the Raman spectra of the conjugated diyne links obtained from graphdiyne before (black curve) and after adsorption (blue curve). After the adsorption of lead ions, a new peak appeared at 2160 cm^{-1} at the shoulder of the C≡C stretching peak (see Figure 2c inset; Figure S4, Supporting Information). Previous works have also reported that when metal ions coordinate to the C≡C bond, the frequency of the C≡C stretching vibration decreases.[37,38] The appearance of a new subpeak at 2160 cm^{-1} in our experiments indicates an interaction between lead ions and the diyne links. Note that in the graphdiyne powder sample we used, only the diyne bonds exposed to the surface participated in the adsorption process and contributed to the redshift of the C≡C stretching peak.

To explore the adsorption performance, the adsorption isotherm of the material was studied and is shown in **Figure 3**a, where the amount of lead ions adsorbed by graphdiyne of a unit weight at different concentrations of lead ions were plotted. The curve was then fitted by the Langmuir isotherm model, which is expressed as

$$q_e = q_{max} K_L C_e / (1 + K_L C_e) \quad (1)$$

where C_e is the equilibrium concentration of lead ions in the aqueous solution (mg L^{-1}); q_e and q_{max} are the amount of lead ions adsorbed on graphdiyne of a unit weight (mg g^{-1}) at concentration C_e and the maximum amount at high equilibrium ion concentration, respectively; and K_L is the Langmuir constant related to the adsorption energy. The fitted Langmuir

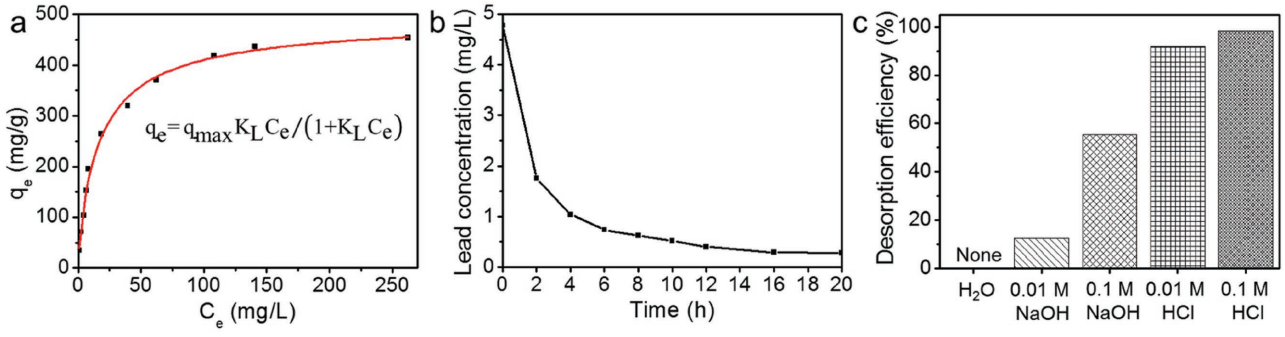

Figure 3. a) Adsorption isotherm of lead ions on graphdiyne. b) Lead ion concentration at different time intervals during adsorption by graphdiyne. c) Desorption efficiency of lead ions from graphdiyne under different conditions.

Table 1. Parameters for the Langmuir model of lead ion adsorption on graphdiyne.

	q_{max} [mg g^{-1}]	K_L	R^2
graphdiyne	470.5	0.07	0.9911

isotherm parameters are listed in **Table 1**. The high value of the correlation coefficient (R^2) indicates that the Langmuir equation fits well with the experimental data, which suggests a monolayer adsorption of lead ions on graphdiyne. The maximum adsorption capacity calculated by the Langmuir isotherm model is 470.5 mg g^{-1}.

Figure 3b shows the lead ion concentration at different time intervals during the adsorption process. Graphdiyne decreased the lead concentration from 4.8 to 1.7 mg L^{-1} in the first 2 h and removed 80% of lead ions from the contaminated water in 4 h. Compared with graphene oxide,[39] the adsorption rate of graphdiyne is relatively low, which is attributed to the porous structure and water insolubility of graphdiyne.

Adsorbents must be regenerable for their practical application in water decontamination. The desorption of lead ions from graphdiyne was investigated under different chemical conditions. Our results show that lead ions adsorbed on graphdiyne can be removed by soaking the graphdiyne powder in acidic or basic solution. The desorption efficiency of lead ions under different conditions is shown in Figure 3c. The desorption efficiency (R(%)) is calculated according to

$$R(\%) = \left(\frac{C_d}{C_o - C_a}\right) \times 100\% \quad (2)$$

where C_o is the initial concentration of lead ions before adsorption; C_a is the concentration of lead ions in water after adsorption; and C_d is the concentration of lead ions released into water after desorption. When lead-ion-adsorbed graphdiyne was added to pure water and stirred for 1 h, no lead ions were released into the water. However, when graphdiyne was immersed in an acidic or basic solution, desorption occurred. The desorption efficiency reached 91.8% in 0.01 M HCl and 98.3% in 0.1 M HCl, which is much higher than that in alkaline solution (12.5% in 0.01 M NaOH and 55.7% in 0.1 M NaOH). Moreover, the Raman peak corresponding to the conjugated diyne links is restored to its original shape after desorption (Figure 2c), further indicating that the change in the Raman peaks is due to the adsorption of lead ions on the acetylenic links.

A graphdiyne-based filter was also fabricated for the purification of water polluted with lead ions. The experimental setup for lead ion filtration is shown in **Figure 4**a. Copper foam, a porous structure composed of an interconnected 3D scaffold of copper with pore diameters of ≈350 µm, was used as the substrate for the growth of graphdiyne (Figure 4b). Before growth, the copper foams were cut into round slices with a thickness of 1 mm and diameter of 20 mm. Graphdiyne was synthesized directly on the surface of the copper and followed the skeletal structure of the copper foam. Experimental details are presented in the Experimental Section in the Supporting Information. A high-magnification SEM image revealed the well-defined and interconnected 3D nanowall structure of graphdiyne (Figure 4c). Five pieces of graphdiyne-based copper foam were stacked together and used as a filter. A certain amount (6 mL) of solution with a lead ion concentration of 4.8 mg L^{-1} was poured over the filter. No applied

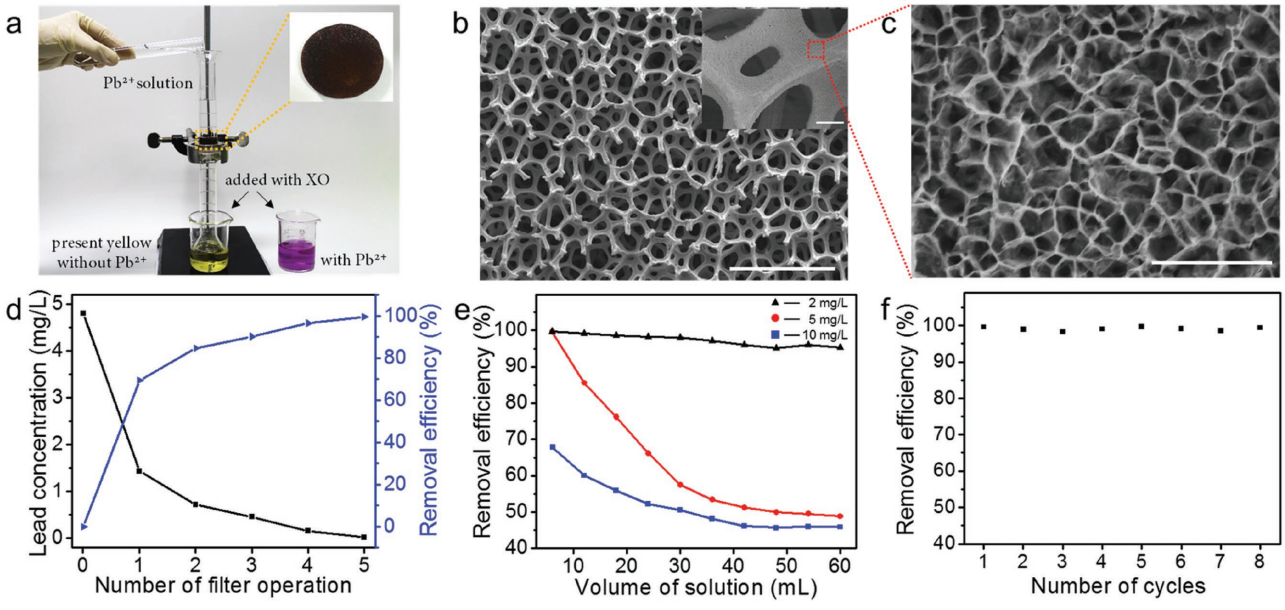

Figure 4. a) Photograph of the experimental setup for lead ion filtration. The solution was dyed with xylenol orange. b) Large-area SEM image of graphdiyne-grown copper foam used for lead ion filtration. Scale bar is 1 mm. Inset: scale bar is 50 µm. c) High-magnification SEM image of the graphdiyne nanowalls grown on copper foam. Scale bar is 1 µm. d) Lead ion concentration of the filtrate and corresponding removal efficiency by graphdiyne after different numbers of filter operations. e) Removal efficiency of lead ions as a function of permeated volume of aqueous solutions with different concentrations of lead ions. f) Cycling performance of the graphdiyne-based foam filters.

pressure is required to achieve filtration. After filtration, the lead ion concentration was reduced to 1.4 mg L^{-1} with a corresponding removal efficiency of 69.4% (Figure 4d). The removal efficiency (E(%)) is calculated using the following equation

$$E(\%) = \left(1 - \frac{C_d}{C_o}\right) \times 100\% \quad (3)$$

where C_o and C_d are the lead ion concentrations of water before and after adsorption, respectively. Thereafter, as the number of filtrations increased, the concentration of lead ions continuously decreased. When the solution was filtered five times, the lead ion concentration was reduced to as low as 0.02 mg L^{-1}, reaching a removal efficiency of 99.6%. The corresponding elemental mapping images of the filter showed that Pb elements are uniformly distributed on the surface of graphdiyne (Figure S5, Supporting Information). The filtration performance was also studied using different volumes and initial lead ion concentrations of the solution (Figure 4e). When the initial lead ion concentration is 2.0 mg L^{-1}, only a slight decrease in the removal efficiency is observed when the volume of the filtered solution reaches 60 mL. In addition, when the initial lead ion concentration is 5.0 or 10.0 mg L^{-1}, the removal efficiency drops to 48.8% or 45.9%, respectively.

To further assess the reliability of the graphdiyne-based copper foam for lead ion filtration, we explored its recyclability performance. In each cycle, the copper foam was washed with 6 mL of 0.1 M HCl after five cycles of filtration of 6 mL of a 5.0 mg L^{-1} lead ion solution and then dried under nitrogen. Over eight repetitions, the removal efficiency of lead ions by the graphdiyne-based copper foam remained at ≈99% (Figure 4f), indicating the good reusability of the filter. The morphology of the filter after eight filtration cycles was also characterized by SEM (Figure S6, Supporting Information). Compared with its initial morphology, the graphdiyne-based filter showed no obvious change, further indicating its good stability.

In summary, graphdiyne was used for the first time to remove lead ions from water. Taking advantage of the interaction between lead ions and acetylenic links, graphdiyne exhibits the effective removal of heavy lead ions from contaminated water. Moreover, a graphdiyne-based filter with high removal efficiency was also fabricated by synthesizing graphdiyne directly on copper foam. The cycling stability and reusability of the filter was demonstrated, indicating that this material is a promising candidate for practical applications in water purification. The adsorption of lead ions on graphdiyne was realized by interactions between the electrons from the metal ions and the p_z or $p_{x/y}$ π/π^* orbitals of the sp-hybridized carbon atoms. Considering this adsorption mechanism, the filter is proposed to have great potential for removing other heavy metal ions from water in a similar manner.

Supporting Information

Supporting Information is available from the Wiley Online Library or from the author.

Acknowledgements

This work was financially supported by the National Natural Science Foundation of China (Grant Nos. 51432002, 51290272, and 21233001) and the Ministry of Science and Technology of China (2016YFA0200101 and 2016YFA0200104).

Conflict of Interest

The authors declare no conflict of interest.

Keywords

adsorption, graphdiyne, ion filtration, lead ions

Received: March 24, 2017
Revised: April 24, 2017
Published online: May 24, 2017

[1] O. Tünay, N. I. Kabdaşli, *Water Res.* **1994**, *28*, 2117.
[2] L. Charerntanyarak, *Water Sci. Technol.* **1999**, *39*, 135.
[3] D. Petruzzelli, R. Passino, G. Tiravanti, *Ind. Eng. Chem. Res.* **1995**, *34*, 2612.
[4] A. Dąbrowski, Z. Hubicki, P. Podkościelny, E. Robens, *Chemosphere* **2004**, *56*, 91.
[5] S. Babel, T. A. Kurniawan, *J. Hazard. Mater.* **2003**, *97*, 219.
[6] K. Jüttner, U. Galla, H. Schmieder, *Electrochim. Acta* **2000**, *45*, 2575.
[7] R. S. Juang, R. C. Shiau, *J. Membr. Sci.* **2000**, *165*, 159.
[8] D. Mohan, C. U. Pittman Jr., *J. Hazard. Mater.* **2006**, *137*, 762.
[9] G. X. Zhao, J. X. Li, X. M. Ren, C. L. Chen, X. K. Wang, *Environ. Sci. Technol.* **2011**, *45*, 10454.
[10] Y.-H. Li, S. G. Wang, J. Q. Wei, X. F. Zhang, C. L. Xu, Z. K. Luan, D. H. Wu, B. Q. Wei, *Chem. Phys. Lett.* **2002**, *357*, 263.
[11] Y.-H. Li, S. G. Wang, Z. K. Luan, J. Ding, C. L. Xu, D. H. Wu, *Carbon* **2003**, *41*, 1057.
[12] M. I. Kandah, J.-L. Meunier, *J. Hazard. Mater.* **2007**, *146*, 283.
[13] M. M. Haley, S. C. Brand, J. J. Pak, *Angew. Chem., Int. Ed. Engl.* **1997**, *36*, 836.
[14] Y. J. Li, L. Xu, H. B. Liu, Y. L. Li, *Chem. Soc. Rev.* **2014**, *43*, 2572.
[15] M. Q. Long, L. Tang, D. Wang, Y. L. Li, Z. G. Shuai, *ACS Nano* **2011**, *5*, 2593.
[16] A. Bhaskar, R. Guda, M. M. Haley, T. Goodson, *J. Am. Chem. Soc.* **2006**, *128*, 13972.
[17] L. Sun, P. H. Jiang, H. J. Liu, D. D. Fan, J. H. Liang, J. Wei, L. Cheng, J. Zhang, J. Shi, *Carbon* **2015**, *90*, 255.
[18] K. Srinivasu, S. K. Ghosh, *J. Phys. Chem. C* **2012**, *116*, 5951.
[19] Y. Jiao, A. Du, M. Hankel, Z. Zhu, V. Rudolph, S. C. Smith, *Chem. Commun.* **2011**, *47*, 11843.
[20] S. W. Cranford, M. J. Buehler, *Nanoscale* **2012**, *4*, 4587.
[21] P. Wu, P. Du, H. Zhang, C. X. Cai, *Phys. Chem. Chem. Phys.* **2014**, *16*, 5640.
[22] S. Lin, M. J. Buehler, *Nanoscale* **2013**, *5*, 11801.
[23] M. Bartolomei, E. Carmona-Novillo, M. I. Hernandez, J. Campos-Martinez, F. Pirani, G. Giorgi, K. Yamashita, *J. Phys. Chem. Lett.* **2014**, *5*, 751.
[24] G. X. Li, Y. L. Li, H. B. Liu, Y. B. Guo, Y. J. Li, D. B. Zhu, *Chem. Commun.* **2010**, *46*, 3256.
[25] R. Matsuoka, R. Sakamoto, K. Hoshiko, S. Sasaki, H. Masunaga, K. Nagashio, H. Nishihara, *J. Am. Chem. Soc.* **2017**, *139*, 3145.

[26] G. X. Li, Y. L. Li, X. M. Qian, H. B. Liu, H. W. Lin, N. Chen, Y. J. Li, *J. Phys. Chem. C* **2011**, *115*, 2611.
[27] J. Y. Zhou, X. Gao, R. Liu, Z. Q. Xie, J. Yang, S. Q. Zhang, G. M. Zhang, H. B. Liu, Y. L. Li, J. Zhang, Z. F. Liu, *J. Am. Chem. Soc.* **2015**, *137*, 7596.
[28] W. B. Wan, M. M. Haley, *J. Org. Chem.* **2001**, *66*, 3893.
[29] N. L. Yang, Y. Y. Liu, H. Wen, Z. Y. Tang, H. J. Zhao, Y. L. Li, D. Wang, *ACS Nano* **2013**, *7*, 1504.
[30] C. S. Huang, S. L. Zhang, H. B. Liu, Y. J. Li, G. T. Cui, Y. L. Li, *Nano Energy* **2015**, *11*, 481.
[31] J. Li, X. Gao, B. Liu, Q. L. Feng, X.-B. Li, M.-Y. Huang, Z. F. Liu, J. Zhang, C.-H. Tung, L.-Z. Wu, *J. Am. Chem. Soc.* **2016**, *138*, 3954.
[32] X. Gao, J. Y. Zhou, R. Du, Z. Q. Xie, S. B. Deng, R. Liu, Z. F. Liu, J. Zhang, *Adv. Mater.* **2016**, *28*, 168.
[33] S. Q. Zhang, J. Y. Wang, Z. Z. Li, R. Q. Zhao, L. M. Tong, Z. F. Liu, J. Zhang, Z. R. Liu, *J. Phys. Chem. C* **2016**, *120*, 10605.
[34] O. J. V. Belleza, A. J. L. Villaraza, *Inorg. Chem. Commun.* **2014**, *47*, 87.
[35] A. Barge, G. Cravotto, E. Gianolio, F. Fedeli, *Contrast Media Mol. Imaging* **2006**, *1*, 184.
[36] J. J. He, S. Y. Ma, P. Zhou, C. X. Zhang, C. Y. He, L. Z. Sun, *J. Phys. Chem. C* **2012**, *116*, 26313.
[37] A. Das, C. Dash, M. A. Celik, M. Yousufuddin, G. Frenking, H. V. R. Dias, *Organometallics* **2013**, *32*, 3135.
[38] J. D. Ferrara, C. Tessier-Youngs, W. J. Youngs, *Organometallics* **1987**, *6*, 676.
[39] Z.-H. Huang, X. Zheng, W. Lv, M. Wang, Q.-H. Yang, F. Kang, *Langmuir* **2011**, *27*, 7558.

